NOTATION

DCF = density of the cyclone feed ($kg \cdot m^{-3}$)
DOF = density of the overflow ($kg \cdot m^{-3}$)
FML = flowrate from the mill ($m^3 \cdot s^{-1}$)
$G(s)$ = matrix transfer function for plant
INA = inverse Nyquist array
j = number $\sqrt{-1}$
MW = feed rate of water to the mill ($kg \cdot s^{-1}$)
PID = proportional, integral and derivative
$PRBS$ = pseudorandom binary sequence
$R(s)$ = rational function used in row operation
$R^*(j\omega)$ = theoretically exact row operator
s = Laplace variable
SF = feed rate of solids ($kg \cdot s^{-1}$)
SW = feed rate of water to the sump ($kg \cdot s^{-1}$)
TOR = torque required to turn the mill (Nm)
ω = frequency ($rad \cdot s^{-1}$)

ACKNOWLEDGMENT

This work, done at the University of Natal, Durban, Republic of South Africa, is published by permission of the Council for Mineral Technology.

LITERATURE CITED

Gault, G. S., W. J. Howarth, A. J. Lynch, and W. J. Whiten, "Automatic control of grinding circuits: theory and practice, *Wld Min.*, **32**, 59 (Nov., 1979).

Rosenbrock, H. H., *Computer-Aided Control System Design*, London, Academic Press (1974).

Rosenbrock, H. H., and C. Storey, *Mathematics of Dynamical Systems*, London, Nelson (1970).

Manuscript received June 29, 1981; revision received February 9, and accepted April 26, 1982.

Disruption Mechanism of Aggregate Aerosol Particles through an Orifice

Based on the drag force of two spheres in contact and the probability density of size ratios of particles which constitute an aggregate particle, the population balance equation describing the change of the particle-size distribution due to the disruption of aggregate particles is derived and the numerical solutions of this equation are obtained.

Experiments were carried out with fly ash particles dispersed in air stream through an orifice at various flow rates. The measured size distributions can be represented by the numerical solutions of the population balance equation.

SHINICHI YUU and TAKASHI ODA

Laboratory of Powder Tech.
Kyushu Institute of Technology
Tobata, Kitakyushu, Japan

SCOPE

Little attention has been focused on the disruption mechanism of agglomerated solid particles in fluid stream (especially in air stream), even when both mechanisms of liquid and solid particle agglomeration and liquid droplet splitting in immiscible liquids have been studied theoretically and experimentally by many authors (for example, Hinze, 1955; Saffman, 1956; Ramabhadran et al. 1976). The reason for this may be the complicated feature of the solid aggregate which consists of particles in contact in which the original particles can be recognized yet. However, reliable estimates of the size distribution of dispersed solid particles in aerosol streams are required in many chemical engineering, for example, in the design of various dust collectors and of atomized fuel injection systems. The principal objective of the present study is to reveal the disruption mechanism of aggregate particles by predicting theoretically the changes of particle-size distribution through an orifice and measuring them experimentally.

Patterson and Kamal (1974) and Kamal and Patterson (1974) studied the shear deagglomeration process of solid agglomerates suspended in viscous liquid. They proposed a model to predict the equilibrium and transient particle-size distributions as a function of shear stress, the initial particle-size distribution and the agglomerate strength distribution. They, however, only treated the deagglomeration process of the agglomerate which consisted of uniform-size particles. Real agglomerate consists of various size particles.

With a view to predicting the manner of break-up of aggregate under fluid forces, Bagster and Tomi (1974) examined the stresses on planes within a sphere in simple flow fields. They assumed that an aggregate is a sphere. The assumption is acceptable for the break-up of droplet, but is not acceptable for the disruption of solid aggregate. Kousaka et al. (1979) proposed the possible disruption mechanisms of aggregate particles in air stream and indicated macroscopically that impaction of particles on some obstacles and acceleration (or deceleration) of aggregates in air stream are effective in aggregate disruption.

In the present study we derive the equation describing the change of the particle-size distribution due to the disruption of aggregate particle, which consists of various size particles, by considering the relative velocity of aggregates to fluid, the drag force of two contact particles and the probability density of size ratios of particles which constitute an aggregate particle, and give the numerical solutions of this equation for various conditions. The changes of the particle-size distributions due to the disruption by the acceleration of aggregate particles through an orifice are measured. The calculated and the measured values are compared, and the disruption mechanism is discussed.

CONCLUSIONS AND SIGNIFICANCE

The population balance equation governing the change of the particle-size distribution due to the disruption of aggregate particles is derived. The results indicate that the disruption force and the possible disruption range of the diameters ratio R of two particles in contact increase with increasing inertia parameter. Therefore, the larger the inertia parameter, the changes of the size distribution and the median diameter due to the disruption by the acceleration increase. The disruption force of aggregate at $R = 1$ is always zero and has a maximum at $R = 2$ when the equispherical diameter is constant. When one attempts to describe the mechanism of the disruption due to acceleration, the most important factors are the inertia parameter of the aggregate and the diameter ratio of particles in contact which the aggregate consists of.

All of the aggregates which can be disrupted under the operating conditions are disrupted at the first orifice and the change of size distribution at the second orifice is negligibly small. Hence, the disruption is almost independent of how many times the aggregates pass through the same size orifices.

Based on this model, the simulation of the disruption process due to acceleration (or deceleration) will permit the prediction of change of the particle-size distribution in the acceleration (or deceleration) flow field.

PREVIOUS WORK

Thomas (1964) studied the turbulent disruption of flocs in liquid suspensions. He showed that under turbulent flow conditions the principal mechanism leading to floc rupture is pressure differences on opposite sides of the floc which cause bulgy deformation and rupture. Patterson and Kamal (1974) dealt with the shear deagglomeration process of solid aggregates suspended in viscous liquid. They proposed a model to predict the equilibrium particle-size distribution as a function of shear stress, the initial particle-size distribution and the aggregate strength distribution. In their model they derived the gain and loss functions of agglomerates through the deagglomeration process. The calculated results based on their model agree with their experimental results within the limitation of experimental and sampling errors. Kamal and Patterson (1974) extended the above-mentioned model to determine the transient particle-size distribution prior to equilibrium in the sheared viscous liquid.

Zahradnicek (1975) summarized various methods of the dispersion of fine powders in air stream. The main method of dispersion is that in which the aerosol stream is passed through a nozzle and a wound tube. Zahradnicek and Löffler (1977) presented the experimental data of the deagglomeration of quartz and limestone fractions with particle size in the range of 0.5 to 10 μm by using their apparatus with an accelerating nozzle and an impact plate. They showed that, if the apparatus with an impact plate is used, a certain amount of crushing of the coarse particles can be no longer avoided when the difference between maximum and the minimum particle size becomes large. Hence, if crushing of the primary particles is not permissible, the apparatus without impact plate is recommended. They also found that even after intensive stressing against the impact plate, some agglomerates which consist mainly of two particles could be found in the aerosol.

Masuda et al. (1977) presented the experimental data of the deagglomeration of calcium carbonate, metallic silicon and talc by using a mixer-type disperser, a fluidized bed, and a capillary pipe. Yamamoto et al. (1977) measured the change of the particle-size distribution of aggregates in air steam through a small pipe by using a cascade impactor. They showed that in such a flow aggregates are disrupted mainly by acceleration of particles. Kousaka et al. (1979) elucidated possible disruption mechanisms of aerosol aggregates and their contributions to disruption by analyzing the disruption forces. They showed macroscopically that impaction of particles on some obstacles and acceleration (or deceleration) of aggregates in air stream are effective in aggregate disruption.

THEORY

Disruption Force

We consider an aggregate which consists of two spherical particles in contact. This aggregate is disrupted to two single particles, if the disruption force becomes stronger than the adhesion force of the aggregate. We consider a multiparticle aggregate which consists of more than two particles as a model aggregate which consists of equispherical two particles in contact. For the unique lumping particles, we assume that the probability density function of the diameter ratio of these equispherical two particles in contact is equal to that of two particle aggregate and that this model aggregate is disrupted to two aggregates which consist of two particles in contact, respectively, and each of them is finally disrupted to two single particles as shown in Figure 1.

The equations of particle motion in the Stokes law regime take the forms.

$$m_1 \frac{du_p}{dt} = 3\pi\beta_1\mu D_1(u_f - u_p) - F_d \quad \text{for particle 1} \qquad (1)$$

$$m_2 \frac{du_p}{dt} = 3\pi\beta_2\mu D_2(u_f - u_p) + F_d \quad \text{for particle 2} \qquad (2)$$

where β_i is a correction factor to account for the effect of the second sphere's presence. Reed and Morrison (1974) gave theoretically the values of β_i for an aggregate motion along their line of centers of two spherical particles in contact. On the calculation we used their values of β_i. Initially, when acceleration is commenced, not all of aggregates will be in an orientation that is applicable to β_i of Reed and Morrison. It is assumed that, if acceleration is continued for a sufficient time, all the aggregates will rotate to the orientation that is applicable to β_i. Equations 1 and 2 reduce to

$$F_d = 3\pi\mu(u_f - u_p)\left(\frac{D_2^3}{D_1^3 + D_2^3}\beta_1 D_1 - \frac{D_1^3}{D_1^3 + D_2^3}\beta_2 D_2\right) \qquad (3)$$

Equation 3 which is similar to that of Kousaka et al. (1977) indicates the disruption force due to the acceleration or the deceleration of two spherical particles in contact. In this paper, we discuss the disruption process due to the acceleration of aggregates through an orifice by using Eq. 3. $(u_f - u_p)$ in Eq. 3 denotes a relative ve-

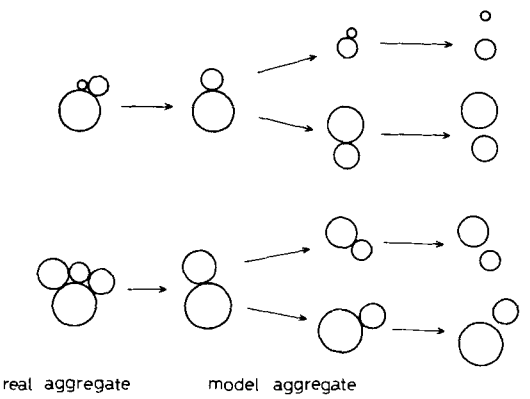

Figure 1. Model aggregate.

locity between fluid and aggregate particle. If the fluid velocity distribution is known, the relative velocity can be calculated by the equation of motion for aggregate particle. As we consider only the centerline region of the orifice flow, the particle motion is one-dimensional. Hence, the equation of motion for the aggregate which consists of two spherical particles is

$$\frac{\pi}{6}\rho_p(D_1^3 + D_2^3)\frac{d^2x}{dt^2} - \frac{3\pi\mu}{C_c}(\beta_1 D_1 + \beta_2 D_2)\left(u\beta_{fx} - \frac{dx}{dt}\right) = 0 \tag{4}$$

Nondimensionalizing Eq. 4 according to Eq. 5, Eq. 6 is obtained.

$$\bar{x} = \frac{x}{d_0},\ \bar{u}_{fx} = u_{fx}/u_{\max},\ \bar{t} = tu_{\max}/d_0 \tag{5}$$

$$\psi'\frac{d^2\bar{x}}{d\bar{t}^2} + \frac{d\bar{x}}{d\bar{t}} - \bar{u}_{fx} = 0,\quad \psi' = \frac{C_c\rho_p D_1^2(1 + R^3)}{18\mu(\beta_1 + \beta_2 R)}\frac{u_{\max}}{d_0} \tag{6}$$

where u_{fx} is a fluid axial velocity distribution on the centerline of the orifice. The absolute value of the maximum relative velocity $|\bar{u}_x - d\bar{x}/d\bar{t}|_{\max}$ in the orifice flow is obtained by the numerical calculation of Eq. 6. On the numerical calculation, the Runge-Kutta-Merson method was used. Substitution of $|\bar{u}_x - d\bar{x}/d\bar{t}|_{\max}$ $u_{\max}$ into $(u_f - u_p)$ of Eq. 3 gives the maximum disruption force for the aggregate through the orifice. The disruption force of a model aggregate which consists of more particles than two are calculated by the same way noted above.

Adhesion Force

In a gaseous medium, particles adhere to each other not only as a result of the London van der Waals force (intermolecular forces), but also the Coulomb interaction, and also under the influence of capillary forces in the liquid condensing in the space between the contiguous particles. The Coulomb force arises between charged particles. Accordingly, if the Coulomb force dominates the particle adhesion, the chain-shaped aggregate particles are formed. The microscope observation of aggregate particles fed to our experimental apparatus showed that there were no chain-shaped aggregate particles. Hence, the Coulomb force might be negligible in our experiment.

In order to rid of the capillary between contiguous particles, the fly ash particles had been dried at 320°C for 24 hours before the experiment. Therefore, we consider only the London van der Waals force between particles as the adhesion force of the aggregate in our disruption model. Hamaker (1937) computed the London van der Waals force between two spherical particles as a function of the diameters.

$$F_v = k\frac{D_1 D_2}{D_1 + D_2},\qquad k = \frac{A}{12a^2} \tag{7}$$

Equation 7 gives adhesion forces of a two-particle aggregate and a model aggregate shown in Figure 1.

Derivation of Population Balance Equation for Disruption Process through an Orifice

We assume that agglomeration of particles and crushing of primary particles do not occur when aerosol particles pass through an orifice. We further assume that the disruption of aggregate particle due to acceleration through an orifice occurs for a much shorter time than that of a particle acceleration through an orifice. Hence, we consider that all of the aggregates which can be disrupted under the operating conditions are disrupted when the aggregate particles pass through the orifice. As a time for a particle acceleration through an orifice is very short, it is unnecessary to consider the usual term of the time dependence of the equation describing the change of the size distribution.

The equispherical diameter ρ of the aggregate, which consists of two spherical particles in contact whose diameters are D_1 and D_2, is

$$\rho^3 = D_1^3 + D_2^3 \tag{8}$$

As we set $D_1 \leqq D_2$ in this paper, the diameter ratio R is

$$R = \frac{D_2}{D_1} \geqq 1 \tag{9}$$

Substitution of Eqs. 8 and 9 into Eqs. 3 and 7 gives the following expressions for the disruption and adhesion forces.

$$F_d = 3\pi\mu|u_f - u_p|\frac{\rho}{\sqrt[3]{1 + R^3}}\left[\beta_1 + \frac{\beta_1 + R\beta_2}{1 + R^3}\right] \tag{10}$$

$$F_v = k\frac{\rho R}{(1 + R)^3\sqrt[3]{1 + R^3}} \tag{11}$$

A range of R in which $F_d \geqq F_v$ is a possible disruption range of R for an arbitrarily chosen aggregate diameter ρ_i. The possible disruption range for various combination of D_1 and D_2 is

$$R(\rho_i)_{\min} \leqq R(\rho_i) \leqq R(\rho_i)_{\max}. \tag{12}$$

If the increase in particle number of D_i particles as a result of disruption of ρ_i particles ($\rho_i \geqq D_i$) is $n^+(D_i, \rho_i)\Delta D_i \Delta\rho_i$ and the decrease as a result of disruption of D_i particles is $n^-(D_i)\Delta D_i$, the following equation is obtained.

$$N_d(D_i)\Delta D_i = N_b(D_i)\Delta D_i + \int_{D_i}^{\infty} n^+(D_i,\rho_i)d\rho_i\Delta D_i - n^-(D_i)\Delta D_i \tag{13}$$

Substitution of Eqs. 8 and 9 into Eq. 12 gives the possible diameter ranges of D_1 and D_2 which are born as a result of disruption of ρ_i particle as follows:

$$\begin{aligned}\frac{\rho_i}{\sqrt[3]{1 + R(\rho_i)^3_{\max}}} \leqq D_1 \leqq \frac{\rho_i}{\sqrt[3]{1 + R(\rho_i)^3_{\min}}}\\ \frac{\rho_i R(\rho_i)_{\min}}{\sqrt[3]{1 + R(\rho_i)^3_{\min}}} \leqq D_2 \leqq \frac{\rho_i R(\rho_i)_{\max}}{\sqrt[3]{1 + R(\rho_i)^3_{\max}}}\end{aligned} \tag{14}$$

If D_i lies in the ranges of Eq. 14, the number of D_i particles increases as the result of disruption of ρ_i particles. The number increment of D_i particles depends upon the probability density distribution of $R(\rho_i)$ for the aggregate particle ρ_i. The number increment of the particles whose diameters lie between $D_i - 1/2\Delta D_i$ and $D_i + 1/2\Delta D_i$ as the result of disruption of all aggregates larger than D_i is

$$\begin{aligned}n^+(D_i)\Delta D_i &= \int_{D_i}^{\infty} n^+(D^i,\rho_i)d\rho_i\Delta D_i\\ &= \int_{D_i}^{\infty} N_b(\rho_i)f_0(\rho_i)\int_{R_1}^{R_2} P(R)dR\,d\rho_i\end{aligned} \tag{15}$$

where $f_0(\rho_i)$ is the number ratio of the aggregates to the aggregates plus single particles whose diameters are ρ_i.

$$\int_{R_1}^{R_2} P(R)dR \fallingdotseq P(R)\Big|_{R=\alpha(\rho_i,D_i)}\Delta R \tag{16}$$

$$\Delta R = \frac{\partial R}{\partial D_i}\Delta D_i \tag{17}$$

Substitution of Eqs. 16 and 17 into Eq. 15 gives

$$n^+(D_i)\Delta D_i = \int_{D_i}^{\infty} BN_b(\rho_i)f_0(\rho_i)P(R)|_{R=\alpha}\frac{\partial R}{\partial D_i}d\rho_i\Delta D_i \tag{18}$$

where if $\rho_i/\sqrt[3]{1 + R(\rho_i)^3_{\max}} \leqq D_i \leqq \rho_i/\sqrt[3]{1 + R(\rho_i)^3_{\min}}$,

$$\frac{dR}{dD_i} = \frac{\sqrt[3]{\rho_i^3 - D_i^3}}{D_i^2}\left(\frac{D_i^3}{\rho_i^3 - D_i^3} + 1\right),\qquad \alpha = \sqrt[3]{\rho_i^3 - D_i^3}/D_i$$

and $B = 1$, and if $\rho_i R(\rho_i)\min/\sqrt[3]{1 + R(\rho_i)^3_{\min}} \leqq D_i \leqq \rho_i R(\rho_i)_{\max}/\sqrt[3]{1 + R(\rho_i)^3_{\max}}$,

$$\frac{dR}{dD_i} = \frac{1}{\sqrt[3]{\rho_i^3 - D_i^3}}\left(\frac{D_i^3}{\rho_i^3 - {}^3_i} + 1\right),$$

$$\alpha = \frac{D_i}{\sqrt[3]{\rho_i^3 - D_i^3}} \text{ and } B = 1.$$

If D_i does not lie in the above ranges, $B = 0$.
If ΔD_i is sufficiently small, it is impossible that both of two particles which are born as a result of disruption lie between $D_i - 1/2\Delta D_i$ and $D_i + 1/2\Delta D_i$, because as will be mentioned later, the disruption force for $R = 1$ is zero.

On the other hand, the number decrease of D_i particles is

$$n^-(D_i)\Delta D_i = N_b(D_i)f_0(D_i)\int_{R(D_i)_{\min}}^{R(D_i)_{\max}} P(R)dR\Delta D_i \quad (19)$$

Substitution of Eqs. 18 and 19 into Eq. 13 gives the population balance equation of particles governing aerosol size distributions for disruption process through an orifice.

$$N_b(D_i)\Delta D_i = N_b(D_i)\Delta D_i + \int_{D_i}^{\infty} BN_b(\rho_i)f_0(\rho_i)P(R) \times \frac{\partial R}{\partial D_i} d\rho_i \Delta D_i - N_b(D_i)f_0(D_i)\int_{R(D_1)_{\min}}^{R(D_i)_{\max}} P(R)dR\Delta D_i \quad (20)$$

The similar way gives the number densities of D_i single and aggregate particles after disruption as follows:

$$N_{ds}(D_i)\Delta D_i = N_b(D_i)(1 - f_0(D_i))\Delta D_i + \int_{D_i}^{\infty} BN_b(\rho_i)f_0(\rho_i)Q(\rho_i)P(R)\left|\frac{\partial R}{\partial D_i}\right|_{R=\alpha} d\rho_i \Delta D_i \quad (21)$$

$$N_{da}(D_i)\Delta D_i = N_b(D_i)f_0(D_i)\Delta D_i + \int_{D_i}^{\infty} BN_b(\rho_i)f_0(\rho_i)(1 - Q(\rho_i))P(R)\left|\frac{\partial R}{\partial D_i}\right|_{R=\alpha} d\rho_i \Delta D_i - N_b(D_i)f_0(D_i)\int_{R(D_1)_{\min}}^{R(D_i)_{\max}} P(R)dR\Delta D_i \quad (22)$$

Hence, the number density of D_i particles after disruption is

$$N_d(D_i) = N_{ds}(D_i) + N_{da}(D_i) \quad (23)$$

Based on the initial values of $N_b(D_i)$, $f_0(\rho_i)$, ($P(R)$ and $Q(\rho_i)$ which were measured, $N_d(D_i)$, $f_0(\rho_i)$ and $Q(\rho_i)$ after the first stage of the disruption through the orifice were calculated numerically by using Eqs. 21 and 22. For the uniqueness of the lumping particles we assumed that $P(R)$ of multiparticle aggregate is equal to that of two-particle aggregate as mentioned earlier.

As will be mentioned later, the experimental probability density distribution $P(R)$ for aggregates is almost unchanged throughout the disruption process. Hence we used the experimental probability density distribution in the upper stream from the orifice.

Then, based on the size distribution, the number ratios after the first stage of the disruption which had been obtained by the above calculation and the measured $P(R)$, the values of the second stage of the disruption were calculated by using the same equations. The process noted above was continued until the change of the size distribution between the nth stage and $(n + 1)$th stage of the disruption did not occur. As mentioned in the preceding section, we consider that all of the aggregates which can be disrupted under the operating conditions are disrupted when the aggregates pass through the orifice. As will be shown in the later section, the calculated results of size distributions converge at about 14th stage. Hence, the number of calculation stage of the results shown in this paper is 14. Both of the diameter divisions ΔD_i and $\Delta\rho_i$ are 0.01 μm, respectively. The numerical integration were performed by using the trapezoidal formula.

EXPERIMENTAL

The experimental set-up is shown in Figure 2. The particles were fed into the steel pipe (Section 2) 50 mm in diameter by a smooth autofeeder (Section 1 of Figure 2) (Taisei Kogyo, type CF-50). The output of the smooth autofeeder was maintained at approximately 0.1 1/h. Fly ash was used for the particles. It was selected as the aerosol particle because its shape is spherical and it is easily dispersed. The larger particles than about 5 μm were collected in the cyclone separator (Section 3). The smaller particles which passed through the steel pipe 50 mm in diameter (Section 4) were suddenly accelerated at the orifice (Section 5). The aerosol particles were sampled at the position A of the pipe centerline before the orifice and the position B of the pipe centerline behind the orifice by the isokinetic sampling method. A brass tube 4 mm in diameter was used as a sampling probe (Section 6). The aerosol particles which were sucked by the sampling probe were enclosed in the cell (Section 7) and the particles were settled on a slide glass set at the bottom of the cell.

The size distribution of the particles on a slide glass was measured with the microscope. The number of the particles which were measured to know a size distribution of aerosol was about 2,000. The orifice diameters were 20 and 30 mm. The air velocities at the pipe centerline far from the orifice were kept at 700 to 1,800 cm/s for these tests. The air velocity distribution at the pipe centerline was measured with a pitot-static probe (2 mm di-

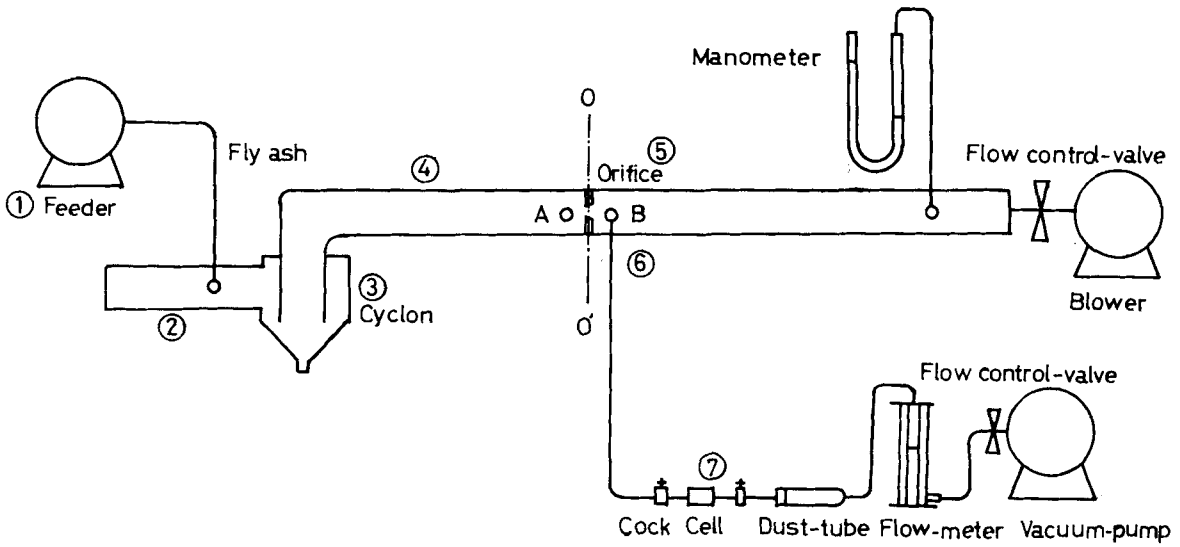

Sampling point	Distance from o-o' (cm)
A	6
B	17.5

Figure 2. Experimental set-up.

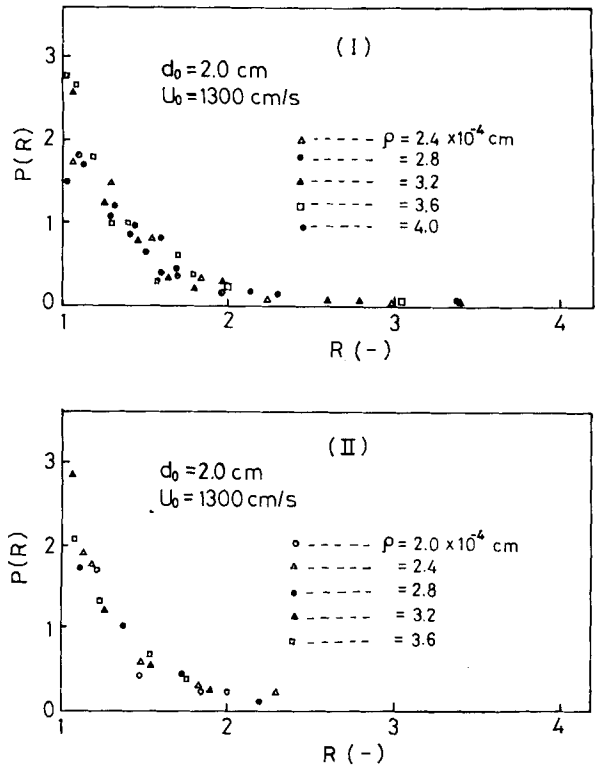

Figure 3. Experimental results of $P(R)$: (I), before the orifice; (II), behind the orifice.

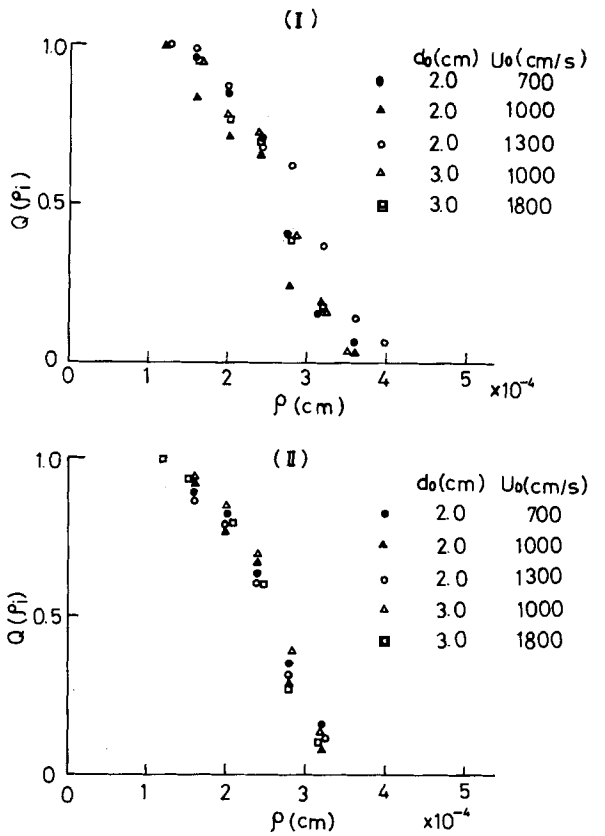

Figure 4. Experimental results of $Q(\rho_i)$: (I), before the orifice; (II), behind the orifice.

ameter). The measurement of particle concentration C_o (0.1 to 1 g/m^3) on the pipe centerline was performed with a photoelectric dust counter (Shibata Kagaku, type S-634) calibrated by the weighing method.

RESULTS AND DISCUSSION

The experimental results of the probability density distribution $P(R)$ for aggregate particle ρ_i which consists of two particles in contact are shown in Figure 3. The data indicate the probability density of R whose equispherical diameters lie between $(\rho - 0.2) \times 10^{-4}$ cm and $(\rho + 0.2) \times 10^{-4}$ cm. Figure 3 shows that $P(R)$ for the large R such as $R = 3$ decreases due to the disruption. However, the whole aspect of $P(R)$ curve is considered almost unchanged throughout the disruption process. Hence, it is acceptable to use $P(R)$ in the upper stream from the orifice for the calculation of Eqs. 21 and 22.

The experimental results of number ratio $Q(\rho_i)$ of aggregates which consist of two particles in contact to all aggregates are shown in Figure 4. It is obvious from Figure 4 that $Q(\rho_i)$ decreases with increasing ρ_i and is almost unchanged throughout the disruption process.

The experimental results of the air velocity distribution at the pipe center-line are indicated in Figure 5. The maximum velocity appears at $x \fallingdotseq d_0$ due to the contraction of the flow. We used the experimental air velocity distribution in Figure 5 for the calculation of the distribution force in the orifice flow.

Figure 6 shows the calculation results of the disruption and the adhesion forces. On the calculation we used $k = 0.48$ which is equivalent to the Hamaker constant $A = 10^{-13}$ and the separation of two particles $a = 1.3 \times 10^{-7}$ cm. Both values for A and a are physically acceptable for an aggregate in air stream.

Figure 6 clearly indicates the range of R where the disruption of aggregate can be occured, i.e., $F_D > F_{vw}$, and it increases with increasing inertia parameter. When $R = 1$, the disruption force is zero. Hence, an aggregate which consists of two equal particles cannot be disrupted by the acceleration (or deceleration). It is worthwhile to note that the disruption force of aggregate for constant equispherical diameter has a maximum at $R = 2$. The shaded

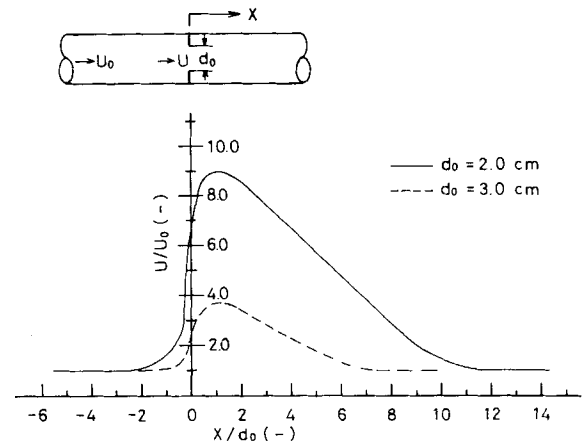

Figure 5. Experimental air velocity distribution on the pipe centerline.

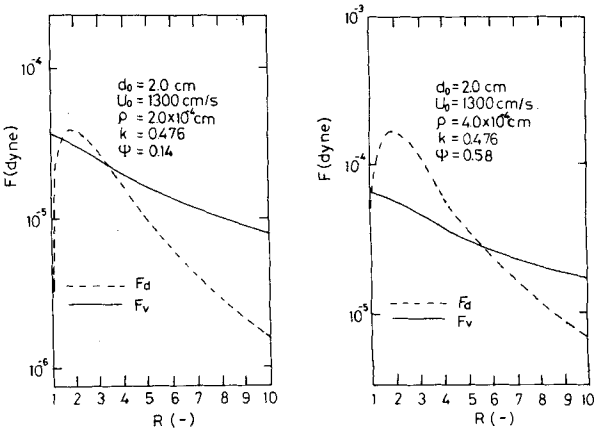

Figure 6. Calculated results of disruption and adhesion forces.

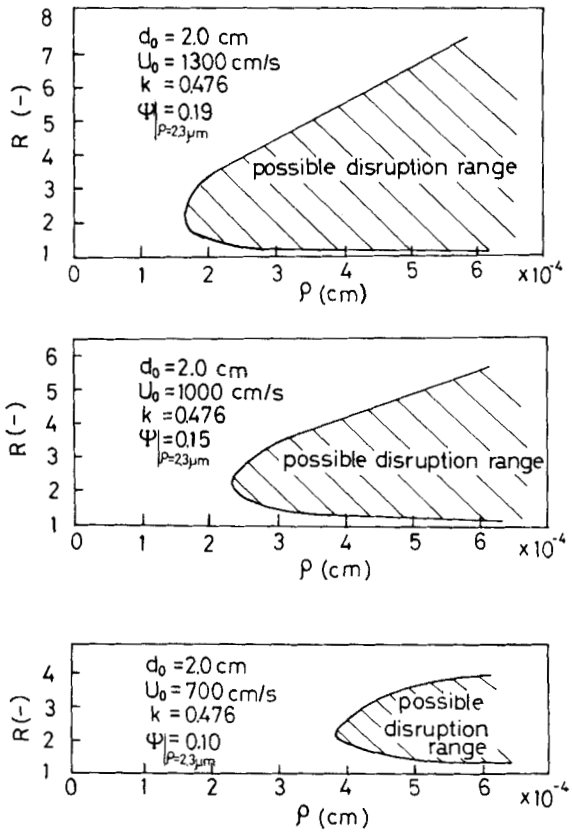

Figure 7. Calculated results of possible disruption ranges of *R*.

portion in Figure 7 shows the calculated results of the possible disruption ranges of R, which increases with increasing a fluid centerline velocity far from an orifice U_0 (or inertia parameter).

Figure 8 shows the experimental results of change of the size distribution of equispherical particles due to the disruption. The symbols ○, △, □, and ● indicate single-, two-, three- and four-particle aggregates, respectively. The number of the aggregates which consist of more than four particles before the disruption was very small.

The experimental and the calculated results of the changes of the particle-size distribution and the median diameter due to the disruption are shown in Figures 9 and 10, respectively. In Figure 9, the symbols ● and x indicate the experimental results of number density distributions of whole particles and single particles before the orifice and the symbols ○ and △ indicate those behind the orifice, respectively. The solid and the dotted lines are the calculated number density distributions of whole particles and single particles, respectively.

The results indicate that the change of the size distribution due to the disruption increases with increasing the inertia parameter based on the averaged particle size before the disruption. The calculated sizes of single particles after the disruption are distributed in larger size range than those of experiment and that on the whole the calculated change of the particle-size distribution is smaller than the experimental one. This seems to be caused by the assumption in our model that an aggregate which consists of more than two particles in contact is disrupted to two aggregates which consist of two particles in contact and that each of them is disrupted to two single particles at the next stage. However in real phenomenon, an aggregate which consists of more than two particles in contact can be disrupted to many single particles at a stretch.

Other problems are: incompleteness of β_i which is a correction factor to account for the effect of the second sphere's presence; and an uncertainty of adhesion forces among particles when an aggregate consists of more particles than two in contact. We used the values of Reed and Morrison (1974) for β_i which is for an aggregate motion along their line of centers of two spherical particles in contact. Some of aggregates still move at arbitrary angle to their line of centers of two particles in contact, even when the maximum relative velocity occurs. β_i for the motion at an arbitrary angle to their line of centers of two particles in contact seems to be larger than that of Reed and Morrison. Both of the incompleteness of β_i and the uncertainty of F_v are the subjects to be solved in the future.

In this model, we have assumed that all of the aggregates which

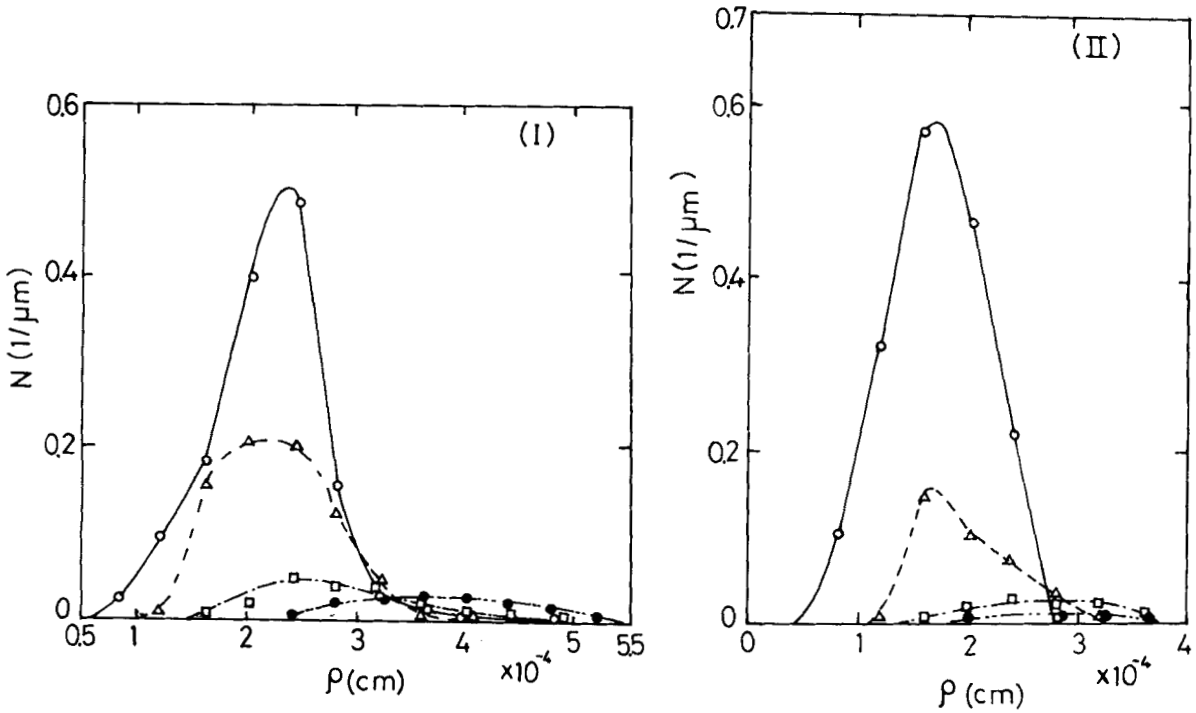

Figure 8. Experimental results of particle number density distributions: (I), before the orifice; (II), behind the orifice (d_0 = 2 cm, U_0 = 1,300 m/s).

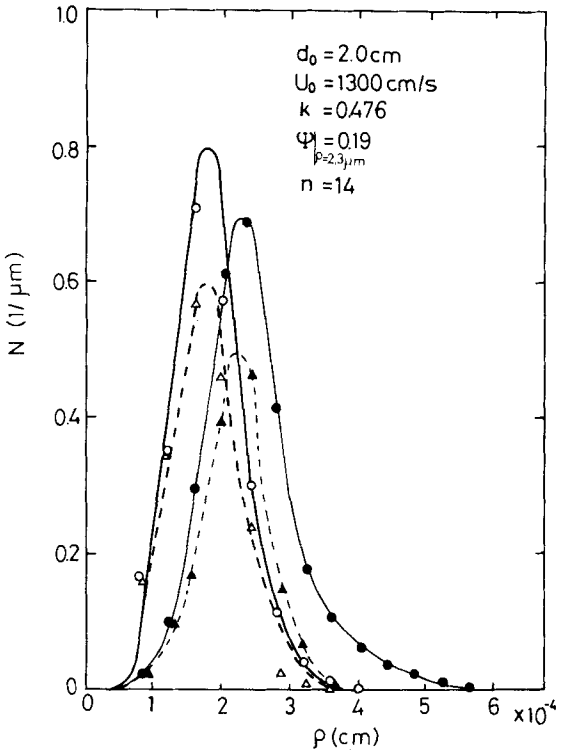

Figure 9a. Comparison of calculated and experimental results of particle number density distributions: (I), before the orifice; (II), behind the orifice.

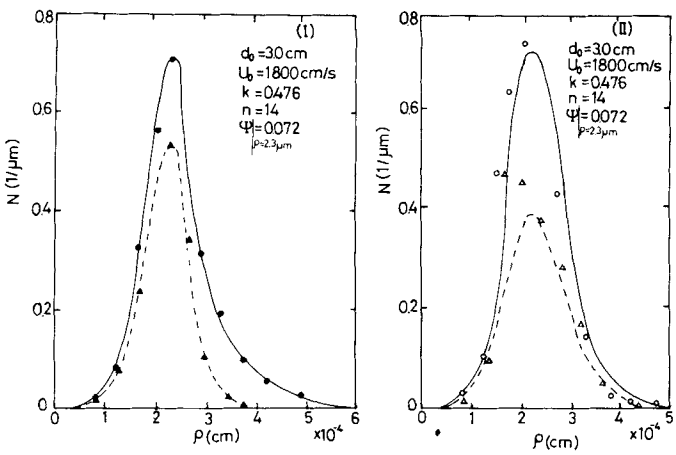

Figure 9b. Comparison of calculated and experimental results of particle number density distributions: (I), before the orifice; (II), behind the orifice.

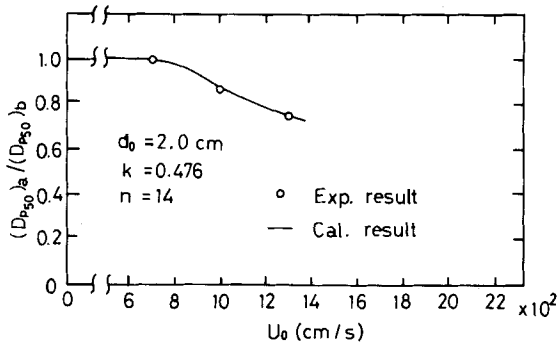

Figure 10. Change of median diameter due to disruption.

can be disrupted under the operating conditions are disrupted when the aggregates are accelerating through the orifice. In order to prove this assumption to be reasonable the change of the size distributions between the two same-sized orifices was measured. The distance between two orifices was 1 m.

Figure 11 shows the measured cumulative-size distributions before and behind each of two orifices. The results indicate that the changes among the size distributions behind the first orifice, before the second orifice, and behind the second orifice are negligibly small. Hence, all of the aggregates which can be disrupted under the operating conditions are disrupted at the first orifice. Therefore, our assumption is reasonable. So, small change between the size distributions behind the first orifice and before the second orifice indicates that the agglomeration does not occur for a distance of 1 m in the pipe flow of this experiment. It infers that the agglomeration in the orifice flow does not occur either.

The normalized changes of the total particle number through the calculation stages, n, of Eqs. 21 and 22 which are mentioned in the previous section are shown in Figure 12. When the number of the calculation stage, n, is larger than about 14, the normalized

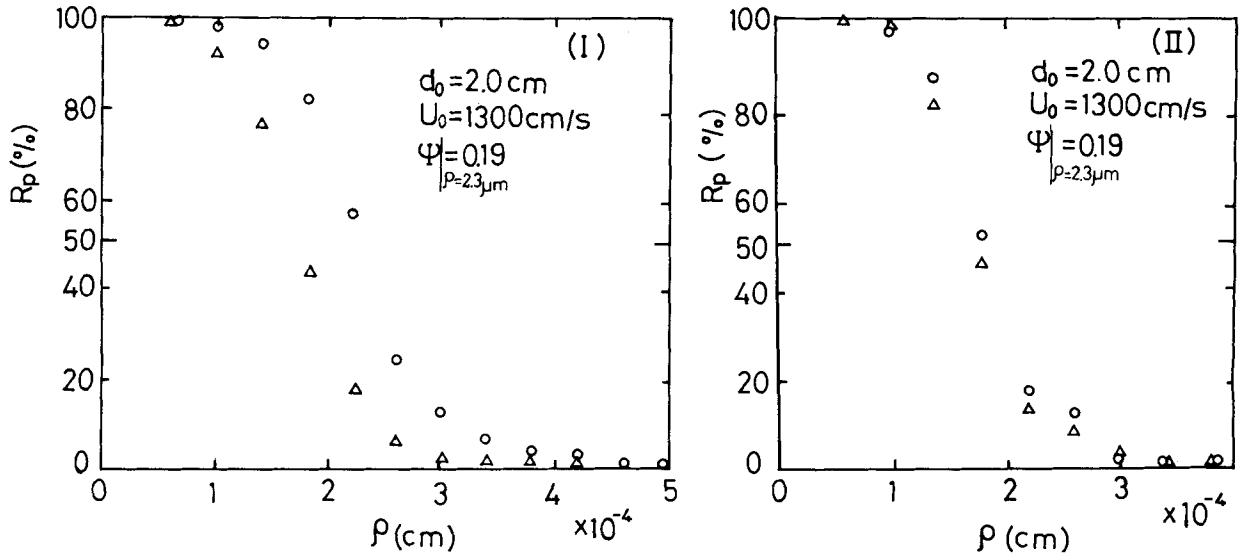

Figure 11. Experimental results of cumulative size distributions. (I): the first orifice, O and △, results before and behind the first orifice; (II), the second orifice, O and △: results before and behind the second orifice.

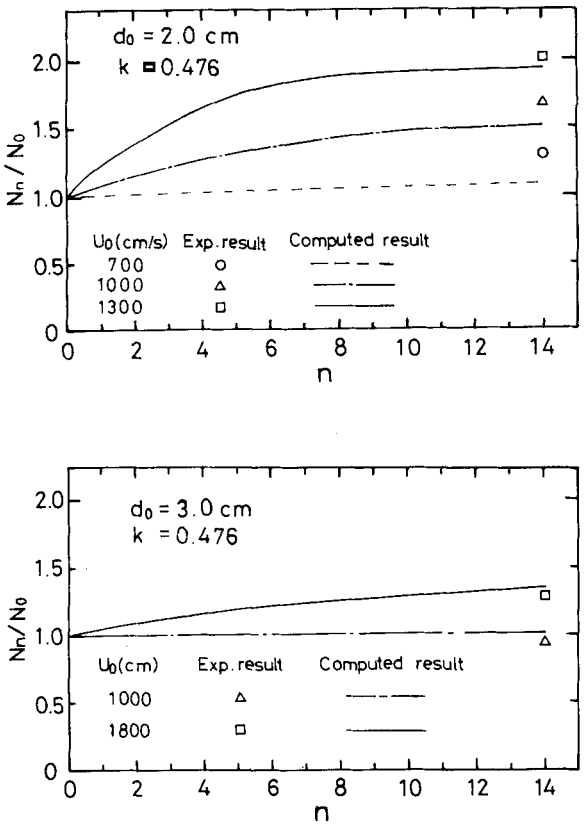

Figure 12. Changes of total particle number through calculation stages *n*.

total particle number converges. The calculated result of the converged total particle number is in fairly good agreement with the experimental total particle number behind the orifice.

NOTATION

A = Hamaker constant, g/s^2
a = separation of two particles in contact, cm
B = constant for discrimination in Eq. 18
C_c = Cunningham's slip correction factor
C_0 = particle concentration, g/m^3
D_i = diameter of i particle, μm
D_{p50} = median diameter based on particle number, μm
$(D_{p50})_a$ = median diameter based on particle number after disruption, μm
$(D_{p50})_b$ = median diameter based on particle number before disruption, μm
d_0 = orifice diameter, cm
F_d = disruption force, g·cm/s^2
F_v = adhesion force, g·cm/s^2
$f_0(\rho_i)$ = number ratio of aggregates to whole particle whose diameters are ρ_i before disruption
m_i = mass of i particle, g
N = frequency of size distribution, $1/\mu$m
$N_b(D_i)$ = number density of D_i particle before disruption, particles/cm^3·μm
$N_d(D_i)$ = number density of D_i particle after disruption, particles/cm^3·μm
$N_{da}(D_i)$ = number density of D_i aggregate particle after disruption, particles/cm^3·μm
$N_{ds}(D_i)$ = number density of D_i single particle after disruption, particles/cm^3·μm
N_0 = total particle number before disruption, particles
N_n = total particle number after disruption, particles
n = calculation stage number
$P(R)$ = probability density of R
$Q(\rho_i)$ = number ratio of two particles aggregates to whole aggregates whose diameters are ρ_i before disruption
R = diameter ratio of two particles in contact
R_p = cumurative size distribution based on particle number
t = time, s
u_{max} = maximum fluid axial velocity, cm/s
U_0 = fluid axial velocity far from orifice, cm/s
u_f, u_p = fluid and particle velocity, respectively, cm/s
x = distance from orifice, m

Greek Letters

β_i = correction factor to account for effect of second particle's presence
ρ_i = equispherical diameter of aggregate, μm
ρ_p = particle density, g/cm^3
μ = fluid viscosity, g/cm·s
ψ' = inertia parameter, $\dfrac{C_c \rho_p D_1^2 (1 + R^3)}{18\mu(\beta_1 + \beta_2 R)} \dfrac{u_{max}}{d_0}$
ψ = inertia parameter, $\dfrac{C_c \rho_p \rho^2 u_{max}}{18\mu d_0}$

LITERATURE CITED

Bagster, D. F., and D. Tomi, "The Stresses within a Sphere in Simple Flow Fields," *Chem. Eng. Sci.*, **29**, 1733 (1974).
Hamaker, H. C., "The London-Van der Waals Attraction between Spherical Particles," *Physica*, **4**, 1058 (1937).
Hinze, J. O., "Fundamentals of the Hydrodynamic Mechanism of Splitting in Dispersion Processes," *AIChE J.*, **1**, 289 (1955).
Kamal, M. R., and I. Patterson, "Transient Deagglomeration of Solid Aggregates in Sheared Viscous Liquids," *Can. J. Chem. Eng.*, **52**, 707 (1974).
Kousaka, Y., K. Okuyama, A. Shimizu, and T. Yoshida, "Dispersion Mechanism of Aggregate Particles in Air," *J. Chem. Eng. Japan*, **12**, 152 (1979).
Masuda, H., S. Fushiro, and K. Iinoya, "Experimental Study on the Dispersion of Fine Particles in Air," *J. Assoc. Powder Tech. Japan*, **14**, 3 (1977).
Patterson, I., and W. R. Kamal, "Shear Deagglomeration of Solid Aggregates Suspended in Viscous Liquids," *Can. J. Chem. Eng.*, **52**, 306 (1974).
Ramabhadran, T. E., T. W. Peterson, and J. H. Seinfeld, "Dynamics of Aerosol Coagulation and Condensation," *AIChE J.*, **22**, 840 (1976).
Reed, L. D., and F. A. Morrison, "The Slow Motion of Two Touching Fluid Spheres along Their Line of Centers," *Inter. J. Multiphase Flow*, **1**, 573 (1947).
Saffman, P. G., and J. S. Turner, "On the Collision of Drops in Turbulent Clouds," *J. Fluid Mech.*, **1**, 16 (1956).
Thomas, D. G., "Turbulent Disruption of Flocs in Small Particle Size Suspension," *AIChE J.*, **10**, 517 (1964).
Yamamoto, H., A. Suganuma, and D. Kunii, "Dispersion of Agglomerated Fine Powder by High Speed Air Stream," *Kagaku Kogaku Ronbunshu*, **3**, 12 (1977).
Zahradnicek, A., "Methoden zur Aerosolherstellung aus Vorgegebenen Festsloffhaufwerken," *Staub Reinhalt. Luft*, **35**, 226 (1975).
Zahradnicek, A., and F. Löffler, "Deagglomeration of Fine Powders in Gas Streams," *Inter. Chem. Eng.*, **19**, 40 (1979).

Manuscript received January 11, 1980; revision received March 31, and accepted April 19, 1982.